

# Modelling and Performance Analysis of the Distributed Scheduler in IEEE 802.16 Mesh Mode

Min Cao  
Dept. Electrical & Computer Engineering  
University of Illinois, Urbana-Champaign  
mincao@uiuc.edu

Wenchao Ma  
Microsoft Research Asia  
t-wenma@microsoft.com

Qian Zhang  
Microsoft Research Asia  
qianz@microsoft.com

Xiaodong Wang  
Dept. Electrical Engineering  
Columbia University  
wangx@ee.columbia.edu

Wenwu Zhu  
Intel China Research Center  
wenwu.zhu@intel.com

## ABSTRACT

To meet the needs of wireless broadband access, the IEEE 802.16 protocol for wireless metropolitan networks (WirelessMAN) has been recently standardized. The medium access control (MAC) layer of the IEEE 802.16 has point-to-multipoint (PMP) mode and mesh mode. Previous works on the IEEE 802.16 have primarily focused on the PMP mode. In the mesh mode, all nodes are organized in an ad hoc fashion and use a pseudo-random function to calculate their transmission time based on the scheduling information of the two-hop neighbors. In this paper, we develop a stochastic model for the distributed scheduler of the mesh mode. With this model, we analyze the scheduler performance under various conditions, and the analytical results match very well with the ns-2 simulation results. The analytical model developed in this paper is instrumental in optimizing the IEEE 802.16 mesh mode system performance. To the best of our knowledge, this work is the first one theoretically investigating the IEEE 802.16 mesh mode scheduling performance.

## Categories and Subject Descriptors

C.2.1 [Computer-Communication Networks]: Network Architecture and Design – *distributed networks, wireless communication*; I.6.5 [Simulation and modeling]: Model development – *modeling methodologies*

## General Terms

Algorithm, Performance

## Keywords

Wireless, 802.16, performance, scheduling, mesh

Permission to make digital or hard copies of all or part of this work for personal or classroom use is granted without fee provided that copies are not made or distributed for profit or commercial advantage and that copies bear this notice and the full citation on the first page. To copy otherwise, to republish, to post on servers or to redistribute to lists, requires prior specific permission and/or a fee.

MobiHoc'05, May 25–27, 2005, Urbana-Champaign, Illinois, USA.  
Copyright 2005 ACM 1-59593-004-3/05/0005 ...\$5.00.

## 1. INTRODUCTION

The IEEE 802.16 standard, “Air Interface for Fixed Broad Wireless Access Systems,” also known as the IEEE WirelessMAN air interface [1], targets at providing last-mile wireless broadband access in metropolitan area networks, delivering performance comparable to traditional cable, DSL or T1 networks [6]. It is designed to evolve as a set of air interfaces based on a common MAC protocol with physical layer specifications dependent on the spectrum of use and the associated regulations. In the standard, the PHY layer employs the orthogonal frequency division multiplexing (OFDM) or single carrier (SC) scheme, and can support a data rate up to 134 Mbit/s in 28 MHz channel.

The IEEE 802.16 MAC protocol has two modes: the point-to-multipoint (PMP) mode and the multipoint-to-multipoint (mesh) mode. In the PMP mode, the nodes are organized into a cellular like structure consisting of a base station (BS) and some subscriber stations (SS). The channels are divided into uplink (from SS to BS) and downlink (from BS to SS), both shared among the SS's. This type of network requires all subscriber stations to be within the transmission range and clear line-of-sight of the BS. On the other hand, in the mesh mode, the nodes are organized in an ad-hoc fashion. All stations are peers and each node can act as routers to relay packets for its neighbors. In typical installations, there still be certain nodes that provide the BS function of connecting the mesh network to backhaul links. However, there is no need to have direct link from SS to the BS of the mesh network. A node can choose the links with the best quality to transmit data; and with an intelligent routing protocol, the traffic can be routed to avoid the congested area. The IEEE 802.16 has two mechanisms to schedule the data transmission in mesh mode – centralized and distributed scheduling. In centralized scheduling, the BS works like a cluster head and determines how the SS's should share the channel in different time slots. Because all the control and data packets need to go through the BS, the scheduling procedure is simple, however the connection setup delay is long. Hence the centralized scheduling is not suitable for occasional traffic needs [5]. In distributed scheduling, every node competes for channel access using a pseudo-random election algorithm based on the scheduling information of the two-hop neighbors. Data subframes are allocated based

on request-grant-confirm three-way handshaking among the nodes. Therefore the distributed scheduling is more flexible and efficient on connection setup and data transmission.

Although the mesh mode exhibits better flexibility and scalability, the distributed channel access control is more complex because every node computes its transmission time without global information. In the 802.16 mesh mode, the control and data channels are separated and every node competes the control channel access. The contentions in the control channel do not affect the current data channel transmission. Therefore, it is impossible to predict the system throughput and delay performance in the mesh mode without understanding the scheduler behavior in control channel thoroughly. In this paper, we focus on the IEEE 802.16 mesh mode and investigate the performance of the distributed scheduling algorithm. To the best of our knowledge, this work is the first one investigating the IEEE 802.16 mesh mode performance. Particularly, we develop a stochastic model to analyze the control channel performance. This model considers the important parameters that could affect the system performance like the total node number, holdoff exponent value, and topology. With this model, the nodes channel contention situation and connection setup time variance can be seen clearly under different parameters. These results are necessary for the whole system optimization. The system throughput and delay performance can also be studied based on the model once the data channel allocation scheme is defined. We also develop an ns-2 simulator for the IEEE 802.16 mesh mode. The theoretical and simulation results match very well.

The remainder of this paper is organized as follows. The distributed scheduling mechanism in the IEEE 802.16 mesh mode is described in Section 2. In Section 3, we propose a stochastic model for assessing the performance (transmission interval and connection setup time) of the distributed scheduler. We provide the ns-2 simulation results and compare them with the analytical performance results in Section 4. Finally, Section 5 contains the conclusions.

## 2. BACKGROUND ON IEEE 802.16 MESH MODE

### 2.1 Related Works

The existing works about the IEEE 802.16 are all on the PMP mode [8, 9, 10]. The IEEE 802.16 mesh mode is more complex because, without any central control, every station competes for the channel in a distributed manner. It is important to understand the system capacity in the mesh mode. There are many existing works on the capacity analysis for general ad hoc networks. In [12, 13, 15, 16, 17], the asymptotic capacity bounds are obtained under the assumption of random topologies. However, the MAC characteristics are not considered hence these bounds can only reveal the scaling behavior of network size on capacity. There is usually a significant gap between the theoretical capacity and the achievable one under some practical MAC protocol.

The IEEE 802.11 also supports ad hoc mode. The performance of ad hoc network based on the IEEE 802.11 is studied in [11, 14, 18, 19, 20, 21, 22, 23], including the node transmission and packet collision probabilities in multi-hop case as well as the hidden terminal effect. However, those performance analysis results for the IEEE 802.11 cannot

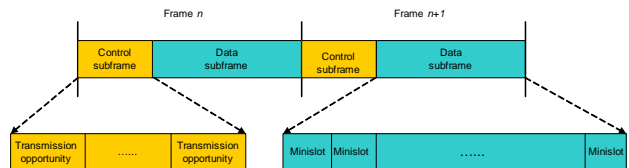


Figure 1: The IEEE 802.16 mesh frame structure

be applied to the IEEE 802.16 mesh mode. The reason is that the two protocols differ in many aspects. For example, the IEEE 802.16 is a slotted system, and all transmissions must be synchronized; whereas in IEEE 802.11 nodes sense the channel before transmission. To reduce collisions caused by hidden terminals, 802.11 uses a four-way RTS/CTS/Data/Ack exchange; whereas 802.16 uses a three-way handshaking to set up connection before data transmission. Unlike 802.11, the control channel and data channel are separated in 802.16 so that the contention in control channel does not affect the current data transmission. Another major difference is that, in 802.16 nodes can reserve multiple slots for the following packets without exchanging control message again; whereas in 802.11, the nodes must compete for the channel for every packet. Because of these differences, a new analytical framework is needed to assess the performance of the 802.16 mesh mode.

### 2.2 IEEE 802.16 Distributed Scheduling Algorithm

In this part, we give a general introduction about the IEEE 802.16 distributed scheduling behavior first. In the 802.16 scheduling algorithm, the control message and data packet are allocated in different time slots in a frame. The allocation of the data time slots is performed through the control message exchange so that there is no contention in the data time slots. In the distributed scheduling, a node selects its next transmission time in the current one. Because other nodes may also transmit in the selected time slot so that the node uses an election algorithm to compute whether it can win or not. If it wins, the node broadcasts its schedule to the neighbors and repeats the procedures in the next transmission time. If it fails, the node selects the next time slot and continues the contention procedures until it wins. For the connection setup, the standard employs a request/grant/confirm three-way handshaking procedure. In the following, the details about the node transmission time calculation, channel contention and connection setup are elaborated. In order to make the scheduling algorithm clear, we need to introduce the frame structure first.

The IEEE 802.16 mesh frame structure is shown in Fig.1. A mesh frame is divided into control and data subframes. There are two control subframe types in mesh mode. One is *network control* that creates and maintains the cohesion between different systems. The other is to coordinate scheduling of data transfers in system, namely, *schedule control*. Frames with the network control subframe occur periodically and all the other frames contain schedule control subframes. Every control subframe consists of sixteen transmission opportunities and every transmission opportunity equals seven OFDM symbols time. The data subframe follows the control subframe in a frame and is divided into min-

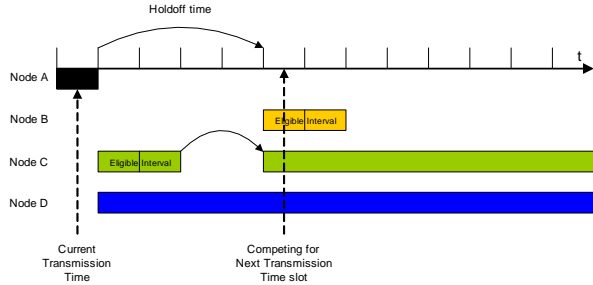


Figure 2: The IEEE 802.16 schedule control sub-frame contention

islots. The minislot is the basic unit for resource allocation. The scheduling message is called MSH-DSCH in the standard. The MSH-DSCH message contains the schedule and data subframe allocation information of the neighborhood. The next transmission time for every station is computed based on such information.

In distributed scheduling, the schedule information for each station is described by two parameters – NextXmtMx and XmtHoldoffExponent. Whenever a station transmits the MSH-DSCH message, it includes these parameters of the neighbors in the message so that every station has the knowledge of the schedule information of its two-hop neighborhood. In the 802.16 mesh mode, the transmission time for a station is an aggregate of some sequential transmission opportunities called eligibility interval spanning a duration of time slots  $2^{XmtHoldoffExponent}$ .  $NextXmtMx < NextXmtTime \leq 2^{XmtHoldoffExponent} \cdot (NextXmtMx + 1)$ . So the eligible interval length for a node is  $2^{XmtHoldoffExponent}$  transmission opportunities. The station can transmit in any slot during this interval. After one eligibility interval, a station must hold off at least  $2^{XmtHoldoffExponent+4}$  transmission opportunities before the next transmission. The holdoff exponent value decides the channel contention time of node so it is an important parameter that can affect the system performance.

In the mesh mode, every station calculates its NextXmtTime during the current transmission time using the *distributed election algorithm* defined in the standard. In this algorithm, one station sets the first transmission slot after the holdoff time as the temporary next transmission opportunity and then competes this slot with all the competing nodes in the two-hop neighborhood as shown in Fig.2. There are three types of competing nodes: (1) nodes whose the Next Xmt Time eligibility interval includes the temporary transmission slot (Node B); (2) nodes whose Earliest Subsequent Xmt Time is the same as or before the temporary slot, where the Earliest Subsequent Xmt Time = Next Xmt Time + Xmt Holdoff Time (Node C); and (3) nodes whose schedules are unknown (Node D). The mesh election algorithm is a pseudo-random function with the slot number and the IDs of all nodes as the inputs. The algorithm generates a series of pseudo-random values based on these inputs. These values are called mixing values in the standard. If the current node ID and the slot number generate the largest mixing value, it wins; otherwise, the current node loses the competition. If the node wins, it sets the temporary

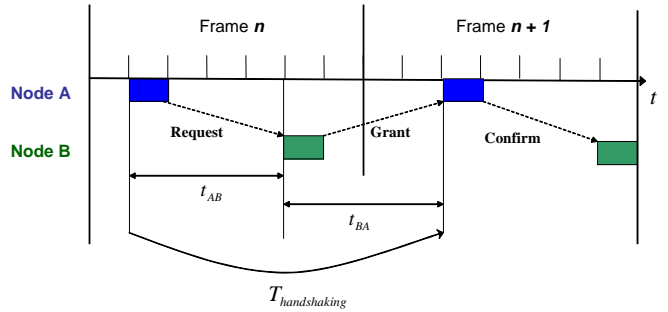


Figure 3: 802.16 mesh three-way handshake

transmission opportunity as its next transmission time, and broadcasts it to the neighbors in the MSH-DSCH packet. If the node loses, it chooses the next transmission opportunity and repeats the above competing procedures until it wins. Based on the above description, we can see that the probability a node winning a contention is determined by the total competing node number, and the competing node number is related with the number of neighbor nodes and their topologies.

The 802.16 distributed mesh scheduler employs a three-way handshaking procedure to set up connections with neighbors. The procedure is shown in Fig.3. The requester sends a request message in the MSH-DSCH packet along with the data subframe availability information. After receiving the request, the receiver responds with a grant message indicating all or a subset of the suggested availabilities that fits the request. Because the MSH-DSCH packet is always broadcasted among the neighborhood, the neighbor nodes not involved in this exchange assume the transmission takes place as granted. When the requester receives the grant message, it transmits a confirmation message to the receiver containing a copy of the granted subframe. Then all the neighbors of the requester cannot use the allocated minislots anymore. Under this mechanism, the neighbors of both the requester and the receiver can have the up-to-date data subframe allocation information.

Based on the description about the IEEE 802.16 mesh scheduler, every node competes for the channel access and tries to broadcast its scheduling information periodically. The channel contention result is correlated with the total node number, exponent value and network topology. In our study, we assume the transmit time sequences of all the nodes in the control subframe form statistically independent renewal processes. Based on this assumption, we develop a stochastic model to estimate the control channel performance.

### 3. MODELLING AND PERFORMANCE ANALYSIS

#### 3.1 Model and Approach

The performance metrics of interest in the MAC layer include the *throughput* and *delay*. In the IEEE 802.16 mesh mode, the details of the data subframe reservation are left unstandardized and to be implemented by the vendors; and

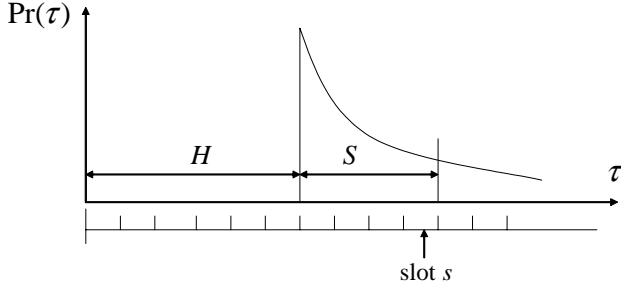


Figure 4: The interval  $\tau$  between two successive transmissions.

the control subframe is independent of the data subframe. We consider the modelling and analysis of the control subchannel, which is characterized by the distributed election algorithm. Assume the number of nodes in the network is  $N$ . Let  $\mathcal{N}_k$  denotes the set of 2-hops neighbor nodes of node  $k$ ,  $N_k = |\mathcal{N}_k|$ ;  $\mathcal{N}_k^{unknown}$  denotes set of nodes whose the schedules are unknown in the neighbor nodes set  $\mathcal{N}_k$ ,  $N_k^{unknown} = |\mathcal{N}_k^{unknown}|$ ;  $\mathcal{N}_k^{known} = \mathcal{N}_k \setminus \mathcal{N}_k^{unknown}$  and  $N_k^{known} = |\mathcal{N}_k^{known}|$ . Let  $x_k$ ,  $k = 1, \dots, N$ , denote the holdoff exponent of node  $k$ , then  $H_k = 2^{x_k+4}$  is the holdoff time of node  $k$ ; and  $V_k = 2^{x_k}$  is the eligibility interval of node  $k$ . Let  $S_k$  denote the number of slots in which node  $k$  fails the competition before it wins, which is a random variable, then the interval between successive transmission opportunities is  $\tau_k = H_k + S_k$ . Our goal is to determine the distributions or mean values of  $\tau_k$  by modelling and analyzing the distributed scheduling algorithm, based on which the *throughput* and *delay* performance can be derived.

Let  $Z_k(t)$  denote the number of transmission times of node  $k$  up to slot  $t$ , then  $Z_k(t)$  is a counting process with inter-event time  $\tau_k$ . To simplify the analysis, we make the following assumptions: (1) the counting process of each node eventually reaches its steady state and the intervals are i.i.d., that is,  $Z_k(t)$  forms a *stationary* and *ergodic* renewal process; and (2) the renewal processes of different nodes are mutually independent at their steady states. Note that the distribution of the renewal intervals of each node depends on the number of competing nodes and their holdoff exponents in its neighborhood. However, when all the processes reach their steady states, we can assume that all the processes are initiated at  $t = -\infty$  and the time of renewal events of different processes are uncorrelated. Our analysis is based on the above assumptions.

The distribution of  $\tau$  is sketched in Fig.4. Suppose the expected number of competing nodes in slot  $s$  for the node of interest is  $M(s)$ . As a result of the pseudo-random election algorithm, the probability that this node wins the slot is

$$p(s) = \frac{1}{M(s)}. \quad (1)$$

So the p.m.f. of  $S$  is

$$P(S = s) = \prod_{i=1}^{s-1} (1 - p(i))p(s), \quad s = 1, 2, \dots \quad (2)$$

To get the distribution of  $\tau_k$ , we need to find  $M_k(s)$ . But  $M_k(s)$  depends on the distributions of  $\tau_j$ ,  $j = 1, \dots, N_k$ ,

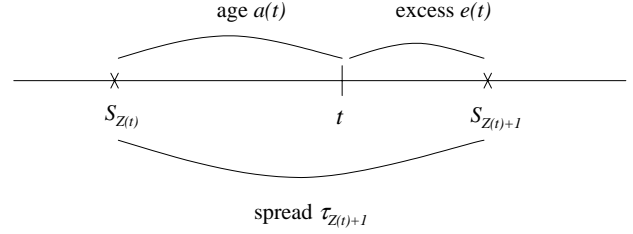


Figure 5: The age and excess time of a renewal process.

since all the nodes in the neighborhood of node  $k$  are candidates to compete with node  $k$ . In this paper, we take the following approach to solve this problem. We will derive  $M_k(s)$  in terms of  $\{p_k(s)\}$  by modelling the distributed election algorithm and then use the relation  $p_k(s) = \frac{1}{M_k(s)}$  to obtain a set of equations for  $\{p_k(s)\}$  to solve them.

### 3.2 Collocated Scenario

To simplify the analysis, we first consider the *collocated* scenario: all nodes are one-hop neighbors of each other. In this simple case, there is no *unknown* node, and  $N_k = N$ ,  $k = 1, 2, \dots, N$ ; that is, all nodes have the same neighborhood.

#### 3.2.1 Identical Holdoff Exponent

To further simplify the analysis, we first assume equal holdoff exponents, i.e.,  $x_1 = x_2 = \dots = x_N$ . Hence when the nodes are collocated, the transmission interval  $\tau_k$  has the same distribution,  $p_k(s) \equiv p(s)$ ,  $s = 1, 2, \dots, \forall k$ .

To proceed with the analysis, we need to introduce the notion of excess time of a renewal process. Let  $Z(t)$  be a renewal process and  $t$  be any chosen time slot, the *spread*,  $\tau_{Z(t)+1}$ , is the renewal interval in which  $t$  lies, as shown in Fig.5. The *age* of the renewal process,  $a(t)$ , is the time since the last renewal before  $t$ ; the *excess* (or residual life time) of the renewal process,  $e(t)$ , is the time to the next renewal after  $t$ . The *limiting distribution of excess time* is established by the following lemma, which is a corollary of the *Renewal Reward Theorem*. The proof is similar to that for the continuous-time version of the lemma in [24].

LEMMA 1. (Limiting Distribution of Excess Time) *Let  $Z(t)$  be a renewal process and  $\tau$  be the renewal interval and  $e(t)$  be the excess time, the limiting distribution of the excess time is  $\lim_{t \rightarrow \infty} \frac{\sum_{s=1}^t I\{e(s) \leq y\}}{t} = \frac{1}{\mu} \sum_{i=1}^y P(\tau \geq i)$  for fixed  $y \geq 0$ , where  $\mu = E[\tau]$  and  $I\{\cdot\}$  is an indicator function.*

By the stationary and ergodic assumption, we can take the limiting distribution of excess time as its stationary distribution

$$P(e \leq y) = \frac{1}{\mu} \sum_{i=1}^y P(\tau \geq i). \quad (3)$$

The distribution of  $\tau$  is given in terms of  $\{p(s)\}$  as

$$P(\tau \geq i) = \begin{cases} 1, & \text{if } i \leq H, \\ \sum_{s=i-H}^{\infty} \prod_{j=1}^{s-1} (1 - p(j))p(s), & \text{if } i > H. \end{cases} \quad (4)$$

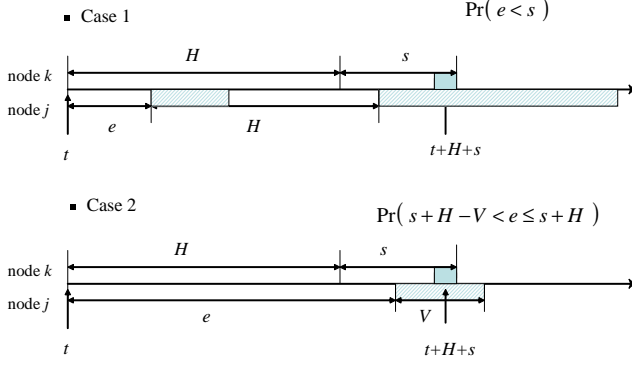


**Figure 6: The competing scenarios of identical holdoff exponent case.**

Using (3) and (4) we have

$$\begin{aligned}
 P(e = y) &= P(e \leq y) - P(e \leq y - 1) = \frac{1}{\mu} P(\tau \geq y) \\
 &= \begin{cases} \frac{1}{\mu}, & \text{if } y \leq H, \\ \frac{1}{\mu} \sum_{s=y-H}^{\infty} \prod_{j=1}^{s-1} (1-p(j)) p(s), & \text{if } y > H. \end{cases} \quad (5)
 \end{aligned}$$

where  $\mu = H + E[S] = H + \sum_{s=1}^{\infty} s \prod_{j=1}^{s-1} (1-p(j)) p(s)$ .

Employing the above results, we can calculate the probability that another node  $j$  will compete with node  $k$  in the given slot  $S_k = s$ . In this simplified scenario, there is no unknown node, the possible competing scenario is either case 1 or case 2, as shown in Fig. 6. Recall that  $H = 2^{x+4}$  is the holdoff time, and  $V = 2^x$  is the eligibility interval length. Since the renewal processes of node  $k$  and node  $j$  are assumed to be statistically independent, at the current transmit time  $t$  of node  $k$ , the time from  $t$  to the next transmit time of node  $j$  is simply the excess time  $e_j(t)$  of node  $j$ . By the assumption that the renewal process is stationary and that the distributions of  $\tau_k$  are identical, we can simply denote  $e_j(t)$  as  $e$ . The competing probability for Case 1 is

$$\begin{aligned}
 &P(\text{EarliestNextXmtTime}_j \leq \text{TempXmtTime}_k) \\
 &= P(t + e + H + 1 \leq t + H + s) = P(e < s). \quad (6)
 \end{aligned}$$

The competing probability for Case 2 is

$$\begin{aligned}
 &P(\text{TempXmtTime}_k \in \text{NextXmtEligibleInterval}_j) \\
 &= P(t + e \leq t + H + s \leq t + e + V - 1) \\
 &= P(s + H - V < e \leq s + H). \quad (7)
 \end{aligned}$$

So the probability that node  $j$  will compete with node  $k$  in the given slot  $S_k = s$  is the sum of the probabilities of the above two cases, and by using (5) we get

$$\begin{aligned}
 &P(\text{node } j \text{ competes with node } k | S_k = s) \\
 &= P(e < s | S_k = s) + Pr(s + H - V < e \leq s + H | S_k = s) \\
 &= \begin{cases} \frac{V}{\mu} + \frac{1}{\mu} \sum_{i=H+1}^{s+H} \sum_{l=i-H}^{\infty} \prod_{j=1}^{l-1} (1-p(j)) p(l), & \text{if } s \leq V, \\ \frac{s}{\mu} + \frac{1}{\mu} \sum_{i=s+H-V+1}^{s+H} \sum_{l=i-H}^{\infty} \prod_{j=1}^{l-1} (1-p(j)) p(l), & \text{if } V < s \leq H, \\ \frac{H}{\mu} + \frac{1}{\mu} \left( \sum_{i=H+1}^s + \sum_{i=s+H-V+1}^{s+H} \right) \cdot \left( \sum_{l=i-H}^{\infty} \prod_{j=1}^{l-1} (1-p(j)) p(l) \right), & \text{if } s > H. \end{cases} \quad (8)
 \end{aligned}$$

When the holdoff exponents of all the nodes are identical, this probability is the same for any two nodes  $k$  and  $j$ . We denote it as  $P(\text{Compete} | S = s)$ , and denote  $N_{\text{compete}}^k(s)$  as the number of nodes (among  $N - 1$  neighbors) which compete with node  $k$  in slot  $s$ . By the assumption of statistical independence,  $N_{\text{compete}}^k(s)$  is binomial distributed, i.e.,  $N_{\text{compete}}^k(s) \sim \mathcal{B}(N - 1, P(\text{Compete} | S = s))$ . Hence the expected number of nodes competing with node  $k$  in slot  $s$  is  $E[N_{\text{compete}}^k(s)] = (N - 1)P(\text{Compete} | S = s)$ , and the competing nodes in slot  $s$  for node  $k$  is

$$M(s) = (N - 1)P(\text{Compete} | S = s) + 1. \quad (9)$$

Substituting (9) into (1) we get

$$p(s) = \frac{1}{M(s)} = \frac{1}{(N - 1)P(\text{Compete} | S = s) + 1}. \quad (10)$$

Combining (8) and (10), we get a set of equations by which we can solve for  $p(s)$ ,  $s = 1, 2, \dots$ . Typically,  $p(s) \rightarrow 0$  as  $s \rightarrow \infty$ , so we can truncate the tail and consider only  $p(s)$ ,  $s = 1, 2, \dots, L$  for some large  $L$ , and then solve the fixed point equations by using standard iterative method. The computation complexity of the above approach is high since there are  $L$  elements to update at each iteration, where  $L$  should be typically chosen large enough. As we will see in the next subsection, this approach becomes more complicated when the holdoff exponents are not identical. This renders it difficult for performance evaluation and impractical for online performance optimization. We next propose a simplified approach by assuming that  $S$  follows a geometric distribution.

By observing the histograms of our simulation data, we find that the distribution of  $S$  can be approximated by a geometric distribution. So we make a further approximation that  $p(1) = p(2) = \dots = p$ , and

$$P(S = s) = (1 - p)^{s-1} p. \quad (11)$$

Then we have  $E[S] = \frac{1}{p}$ . Similar to (4) and (5) we can derive the distribution of  $\tau$  as follows

$$P(\tau \geq y) = \begin{cases} 1, & \text{if } y \leq H, \\ (1 - p)^{y-H-1}, & \text{if } y > H; \end{cases} \quad (12)$$

and the distribution of  $e$  as

$$\begin{aligned}
 P(e = y) &= \frac{1}{\mu} P(\tau \geq y) \\
 &= \begin{cases} \frac{1}{\mu}, & \text{if } y \leq H, \\ \frac{1}{\mu} (1 - p)^{y-H-1}, & \text{if } y > H. \end{cases} \quad (13)
 \end{aligned}$$

Then the probability that another node  $j$  will compete with node  $k$  in the given slot  $S_k = s$  is

$$\begin{aligned}
 &P(\text{node } j \text{ competes with node } k | S_k = s) \\
 &\triangleq P(\text{Compete} | S = s) = P(e < s | S_k = s) \\
 &+ P(s + H - V < e \leq s + H | S_k = s) \\
 &= \begin{cases} \frac{V}{\mu} + \frac{1-(1-p)^s}{\mu p}, & \text{if } s \leq V, \\ \frac{s}{\mu} + \frac{(1-p)^{s-V} - (1-p)^s}{\mu p}, & \text{if } V < s \leq H, \\ \frac{H}{\mu} + \frac{1-(1-p)^{s-H-1} + (1-p)^{s-V} - (1-p)^s}{\mu p}, & \text{if } s > H. \end{cases} \quad (14)
 \end{aligned}$$

For the geometric distribution,  $p(s) = p$  for all  $s$ , hence  $M(s) = M$  for all  $s$ , which implies that the number of competing nodes in each slot  $s$  should be the same. Here we

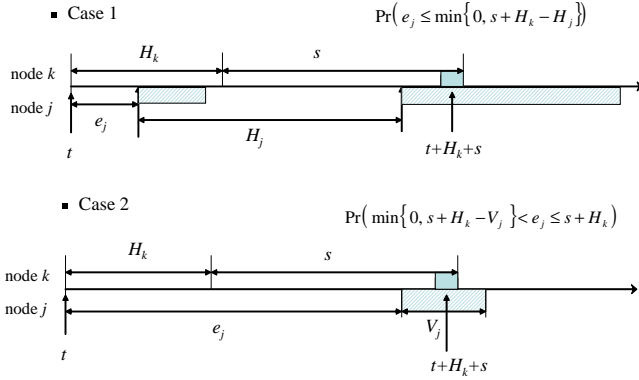


**Figure 7: The competing scenarios of nonidentical holdoff exponents case.**

approximate  $M$  as the expectation of  $M(s)$  as

$$\begin{aligned} \frac{1}{p} &= M \simeq E_S[M(s)] \\ &= E_S[(N-1)P(\text{Compete}|S=s) + 1]. \end{aligned} \quad (15)$$

Using (14) and (15) and after some manipulations, we get

$$\frac{1}{p} = (N-1) \left( \frac{V}{\mu} + \frac{1}{\mu p} - \frac{(1-p)^{V+1} - (1-p)^{H+2}}{\mu p(2-p)} \right) + 1. \quad (16)$$

Notice that the last term in the second bracket of RHS is typically small, we can simplify (16) by dropping that term as

$$\frac{1}{p} \simeq (N-1) \left( \frac{V}{\mu} + \frac{1}{\mu p} \right) + 1. \quad (17)$$

Substitute  $E[S] = \frac{1}{p}$ , and  $\mu = H + E[S]$  into (17), we express the above equation in terms of  $E[S]$  as

$$E[S] = (N-1) \frac{V + E[S]}{H + E[S]} + 1 = (N-1) \frac{2^x + E[S]}{2^{x+4} + E[S]} + 1. \quad (18)$$

A fixed point iteration can be used to obtain  $E[S]$  from (18).

### 3.2.2 Nonidentical Holdoff Exponents

Now we consider the case where holdoff exponents  $x_k$ ,  $k = 1, \dots, N$  are not identical, but we still restrict ourselves to the collocated scenario. The analysis is similar to the identical holdoff exponent case. The competing scenarios are illustrated in Fig.7. The competing probability for Case 1 is

$$\begin{aligned} &P(\text{EarliestNextXmtTime}_j \leq \text{TempXmtTime}_k) \\ &= P(t + e_j + H_j \leq t + H_k + s) \\ &= P(e_j \leq \min\{0, s + H_k - H_j\}). \end{aligned} \quad (19)$$

And the competing probability for Case 2 is

$$\begin{aligned} &P(\text{TempXmtTime}_k \in \text{NextXmtEligibleInterval}_j) \\ &= P(t + e_j \leq t + H_k + s \leq t + e_j + V_j) \\ &= P(\min\{0, s + H_k - V_j\} < e_j \leq s + H_k). \end{aligned} \quad (20)$$

Denote  $P(C_k^j | S_k = s)$  as the probability that node  $j$  will compete with node  $k$  in the given slot  $S_k = s$ , which is given

by

$$\begin{aligned} &P(C_k^j | S_k = s) \\ &\triangleq P(\text{node } j \text{ competes with node } k | S_k = s) \\ &= P(e_j < \min\{0, s + H_k - H_j\}) \\ &\quad + P(\min\{0, s + H_k - V_j\} < e_j \leq s + H_k) \\ &= \begin{cases} P(e_j \leq s + H_k | S_k = s) = \frac{s + H_k}{\mu_j}, & \text{if } s + H_k \leq V_j, \\ P(s + H_k - V_j < e_j \leq s + H_k | S_k = s) = \frac{V_j}{\mu_j}, & \text{if } V_j < s + H_k \leq H_j, \\ P(e_j < s + H_k - H_j | S_k = s) \\ \quad + P(s + H_k - V_j < e_j \leq s + H_k | S_k = s) = (*), & \text{if } s + H_k > H_j. \end{cases} \end{aligned} \quad (21)$$

where  $\mu_j = H_j + E[S_j] = H_j + \sum_{s=1}^{\infty} s \prod_{i=1}^{s-1} (1 - p_j(i)) p_j(s)$ , and  $(*)$  is expressed as

$$\begin{aligned} (*) &= P(e_j < s + H_k - H_j | S_k = s) \\ &\quad + P(s + H_k - V_j < e_j \leq s + H_k | S_k = s) \\ &= \begin{cases} \frac{V_j}{\mu_j} + \frac{1}{\mu_j} \sum_{y=H_j+1}^{s+H_k} \sum_{l=y-H_j}^{\infty} \\ \quad \cdot \prod_{i=1}^{l-1} (1 - p_j(i)) p_j(l), & \text{if } H_j < s + H_k \leq H_j + V_j, \\ \frac{s+H_k-H_j}{\mu_j} + \frac{1}{\mu_j} \sum_{y=s+H_k-V_j+1}^{s+H_k} \sum_{l=y-H_j}^{\infty} \\ \quad \cdot \prod_{i=1}^{l-1} (1 - p_j(i)) p_j(l), & \text{if } H_j + V_j < s + H_k \leq 2H_j, \\ \frac{H_j}{\mu_j} + \frac{1}{\mu_j} \left( \sum_{y=H_j+1}^{s+H_k-H_j} + \sum_{y=s+H_k-V_j+1}^{s+H_k} \right) \\ \quad \cdot \left( \sum_{l=y-H_j}^{\infty} \prod_{i=1}^{l-1} (1 - p_j(i)) p_j(l) \right), & \text{if } s + H_k > 2H_j. \end{cases} \end{aligned} \quad (22)$$

Again by the assumption of statistical independence,  $M_k(s) = \sum_{j \neq k, j=1}^N P(C_k^j | S_k = s) + 1$ , and we have

$$p_k(s) = \frac{1}{M_k(s)} = \frac{1}{\sum_{j \neq k, j=1}^N P(C_k^j | S_k = s) + 1}. \quad (23)$$

Similarly we can find the distributions of  $\tau_j$ ,  $j = 1, 2, \dots, N$  by the fixed point iterations.

Due to the complexity of the above approach, as before we further assume that  $S_j$ ,  $j = 1, 2, \dots, N$  are geometrical distributed, that is, assume  $p_j(1) = p_j(2) = \dots \triangleq p_j$ , and

$$P(S_j = s) = (1 - p_j)^{s-1} p_j. \quad (24)$$

Hence the distribution of  $e_j$  is

$$\begin{aligned} P(e_j = y) &= \frac{1}{\mu_j} P(\tau_j \geq y) \\ &= \begin{cases} \frac{1}{\mu_j}, & \text{if } y \leq H_j, \\ \frac{1}{\mu} (1 - p_j)^{y-H_j-1}, & \text{if } y > H_j. \end{cases} \end{aligned} \quad (25)$$

Then (22) can be simplified as

$$\begin{aligned}
(*) &= P(e_j < s + H_k - H_j | S_k = s) \\
&+ P(s + H_k - V_j < e \leq s + H_k | S_k = s) \\
&= \begin{cases} \frac{V_j + \frac{1-(1-p_j)^{s+H_k-H_j}}{\mu_j p_j}}{\mu_j}, & \text{if } H_j < s + H_k \leq H_j + V_j, \\ \frac{(1-p_j)^{s+H_k-H_j-V_j} - (1-p_j)^{s+H_k-H_j}}{\mu_j p_j}, & \text{if } H_j + V_j < s + H_k \leq 2H_j, \\ \frac{H_j + \frac{1-(1-p_j)^{s+H_k-2H_j+(1-p_j)^{s+H_k-H_j-V_j}}}{\mu_j p_j}}{\mu_j}, & \text{if } s + H_k > 2H_j. \end{cases} \quad (26)
\end{aligned}$$

To estimate  $p_k$ , we proceed as follows

$$\begin{aligned}
\frac{1}{p_k} &= M \simeq E_{S_k}[M_k(s)] \\
&= \sum_{j \neq k, j=1}^N E_{S_k} \left[ P(C_k^j | S_k = s) \right] + 1. \quad (27)
\end{aligned}$$

We can derive  $E_{S_k} [P(C_k^j | S_k = s)]$  from (21), (24) and (26). The formulation is very complex and takes different forms depending on the value of  $x_k$  and  $x_j$ . Similarly we can make some approximations to find the counterparts of (18) as in the last subsection. Here we directly give the approximation result as

$$E_{S_k} \left[ P(C_k^j | S_k = s) \right] \simeq \begin{cases} \frac{V_j + E[S_k]}{\mu_j}, & \text{if } x_j \geq x_k, \\ 1, & \text{if } x_j < x_k. \end{cases} \quad (28)$$

Note that  $E[S_k] = \frac{1}{p_k}$ , combining (27) and (28), we have

$$\begin{aligned}
E[S_k] &= \sum_{j=1, j \neq k, x_j \geq x_k}^N \frac{2^{x_j} + E[S_k]}{2^{x_j+4} + E[S_j]} \\
&+ \left( \sum_{j=1, j \neq k, x_j < x_k}^N 1 \right) + 1, \quad k = 1, \dots, N. \quad (29)
\end{aligned}$$

Again we can solve for  $E[S_k]$ 's using fixed point iteration.

### 3.3 General Topology Scenario

Now we extend the results to the *general topology* scenario. The difference between the collocated scenario and the general topology scenario is that in the general topology: (1) the neighborhood node sets of different nodes  $\mathcal{N}_k$  may be different; (2) there exist unknown nodes, hence besides the competing cases 1 and 2, there are unknown competing nodes. However, the analysis procedure is almost the same for each node, (27) still holds with minor modifications

$$E[S_k] = \frac{1}{p^k} \simeq \sum_{j \neq k, j=1}^{N_k} E_{S_k} \left[ P(C_k^j | S_k = s) \right] + 1, \quad (30)$$

where  $N_k = N_k^{\text{known}} + N_k^{\text{unknown}}$ . Since unknown nodes are always regarded as competing nodes in each slot by the

distributed election algorithm, we have

$$\begin{aligned}
&Pr(C_j^k | S_k = s) \\
&= P(j \text{ compete with } k \text{ in slot } s | S_k = s) \\
&= 1, \quad j \in \mathcal{N}_k^{\text{unknown}}, \forall s \quad (31)
\end{aligned}$$

Taking unknown nodes into account, we find the expression for  $E[S_k]$  by a similar procedure as in the last section

$$\begin{aligned}
E[S_k] &= \sum_{j=1, j \neq k, x_j \geq x_k}^{N_k^{\text{known}}} \frac{2^{x_j} + E[S_k]}{2^{x_j+4} + E[S_j]} \\
&+ \left( \sum_{j=1, j \neq k, x_j < x_k}^{N_k^{\text{unknown}}} 1 \right) + N_k^{\text{unknown}} + 1, \\
&k = 1, \dots, N. \quad (32)
\end{aligned}$$

Again we can solve for  $E[S_k]$ 's by fixed point iterations.

### 3.4 Performance Metrics Estimation

Let  $T_{handshake}^{AB}$  denotes the time node  $A$  needs to accomplish a three-way handshaking with node  $B$ . Now we can derive  $E[T_{handshake}^{AB}]$  given the distributions of  $\tau_k$  of all nodes  $k = 1, \dots, N$ . From the procedure of the three-way handshaking as illustrated in Figure 3, we can see that  $T_{handshake}^{AB} = t_{AB} + t_{BA}$ , where  $t_{AB}$  is the time interval between node  $A$  sending a *Request* to  $B$  and  $B$  replying a *Grant* to  $A$ , and  $t_{BA}$  is the time interval between  $B$  sending the *Grant* and  $A$  replying with a *Confirm*. By the independence assumption, and further assuming that the renewal processes of node  $A$  and  $B$  have run for a long time so that we can assume that  $t_{AB}$  follows a limiting distribution as the excess time  $e_B$ . However,  $t_{BA}$  may not follow the same distribution as  $e_A$  since it is dependent on  $t_{AB}$ , thus the limiting distribution does not hold. It is very complicated to find the exact distribution of  $t_{BA}$  since the renewal interval  $\tau$  is not geometrical distributed. Hence we take an empirical approach here. Note that when  $\tau_A \ll \tau_B$ , the renewal process of node  $A$  can be considered to run for a long time after sending *Request*, so in this case we can assume that  $t_{BA} \simeq e_A$ . In this case,  $E[T_{handshake}^{AB}] \simeq E[e_B] + E[e_A]$ . On the other hand, when  $\tau_A \gg \tau_B$ ,  $t_{BA} \simeq \tau_A$  since the portion of excess time  $e_B$  is negligible, and  $E[T_{handshake}^{AB}] \simeq E[e_B] + E[\tau_A] = E[e_B] + \mu_A$ . Empirically, we can estimate  $E[T_{handshake}^{AB}]$  as

$$E[T_{handshake}^{AB}] \simeq E[e_B] + \alpha \mu_A + (1 - \alpha) E[e_A] \quad (33)$$

where  $\alpha$  is a compromising factor. Based on the simulation data, we find  $\alpha = \frac{E[S_A]}{\mu_A}$  to be a good choice for the identical holdoff exponent case and  $\alpha = \left( \frac{\mu_A}{\mu_A + \mu_B} \right)^2$  for the nonidentical holdoff exponents case. Once  $E[S_k]$  is known, from (25) we can calculate  $E[e_k]$  as

$$\begin{aligned}
E[e_k] &= \sum_{y=1}^{H_k} \frac{y}{\mu_k} + \sum_{y=H_k+1}^{\infty} \frac{y}{\mu_k} (1-p^k)^{y-H-1} \\
&= \frac{H_k(H_k+1)}{2\mu_k} + \frac{H_k}{\mu_k p^k} + \frac{1}{\mu_k p^{k^2}} \\
&= \frac{2^{x_k+3} + 2^{2x_k+7} + 2^{x_k+4} E[S_k] + E^2[S_k]}{2^{x_k+4} + E[S_k]}. \quad (34)
\end{aligned}$$

Employing the results of  $E[S_k]$ 's from previous subsections, we can determine  $E[T_{handshake}^{AB}]$  for any two neighbor nodes A and B by using (33) and (34). Note that  $E[T_{handshake}]$  is simply the MAC *delay* performance metric. To evaluate the MAC *throughput* performance, we need to know the data subframe reservation mechanism, which is left unspecified in the standard and open for implementation. However, the above analysis results for the control channel are necessary for determining the throughput performance once the data reservation mechanism is specified.

## 4. SIMULATION RESULTS

In this section, we provide ns-2 simulation results for various scenarios and compare them with the analytical performance predicted by the modelling framework developed in this paper.

### 4.1 Simulation Setup

We first outline the structure of our ns-2 simulator. The ns-2 simulator used in our study includes typical TCP/IP/LL/MAC/PHY stack. The current MAC modules for ns-2 include 802.11, ethernet, TDMA and satellite; however, no 802.16 MAC module is available. In our work, we implement a new MAC module for the IEEE 802.16 mesh mode and use it to study the system performance. The module consists of three logic parts, the network controller, the scheduling controller, and the data channel component. The network controller is responsible for the network configuration, node entry, synchronization, etc. In real systems, the network controller is very complex; in our simulator, we simplify this part by keeping the network configuration message exchange mechanism and ignoring the message contents. The scheduling controller part handles the signaling channel contention, three-way handshaking and data channel allocation. During the holdoff time of a node, the MSH-DSCH messages received from PHY module are sent to the scheduling controller. In the transmission slot, the scheduling controller contends the next transmission time using the election algorithm defined in the standard based on the collected neighbors' information. A new timer is set to activate the next transmission after that. Besides the scheduling, the scheduling controller also sets the *request* field properly in the MSH-DSCH message if data packets are received from LL layer and replies with *grant* or *confirm* according to the three-way handshaking procedure. The data channel component receives and transmits data packets in the allocated time slots. In our simulation we use a simple reservation mechanism by assigning each data packet in one minislot.

The exponent value determines the node transmission interval and holdoff time. In our simulations, the set of possible exponent values is  $\{0, 1, 2, 3, 4\}$ . During initialization, every node obtains a random node ID. The initial transmission time for each node is arranged sequentially. In the mesh mode, the node IDs are the input parameters of the election algorithm. The randomness of the node IDs makes sure the initial transmission time arrangement does not affect the final results. In our simulation, we investigate two types of network topologies, namely, collocated and general scenarios.

#### 4.1.1 Collocated Scenario

In the collocated scenario, all nodes are within the radio transmission range of each other so that every node can ob-

tain the up-to-date schedule information of all neighbors. The IEEE 802.16 is a new standard and lacks of field testing. The total transmission opportunities in control channel becomes 256 when the exponent value is 4. On choosing the exponent value, we believe 4 is large enough; otherwise, the connection setup latency will become too long. So we set 4 to be the largest exponent value in our simulations. Besides the exponent values, we also vary the total node number to study the control channel performance.

There are two cases in the collocated scenario – identical and nonidentical exponent. In the first case, all the nodes have same exponent values. In the second case, different node may have different exponent values and the node numbers with different exponent values are equal. The reason to have the two cases is that the consecutive transmission interval, especially the connection setup delay are affected by the exponent values of the competing neighbors.

#### 4.1.2 General Topology

In the IEEE 802.16 mesh mode, nodes store the scheduling information of all nodes in two-hop neighborhood. In the general topology, the scheduling information of some neighbors beyond one hop may become stale. The reason is that some one-hop neighbors could not update the information in time for some specific transmission order. During the current transmission time, a node can tell the stale scheduling information by comparing those nodes' schedules with the current time. These nodes become *unknown* nodes because the local node does not know their actual scheduling information and always treats them as potential competitors (Node D in Fig.2). So, in the general topology, the potential competing nodes number for a node differs from that in the collocated scenario.

In our simulation, the node placement in general topology is shown in Fig.8. There are totally 15 nodes and the one-hop neighbors are connected by lines. The exponent values for the nodes are not identical. Their exponent values are assigned arbitrarily from set  $\{0, 1, 2, 3, 4\}$  and listed in table 1. In this topology, we assign a node between two nodes with smaller exponent values a larger exponent value. The node with larger exponent value has longer update period so that the scheduling information of the two nodes with smaller exponent values has more opportunities becoming stale to each other. In the simulation, if a local node finds the stored schedule for a node within the two-hop neighborhood is out-of-date, the local node treats it as an *unknown* node and contends its next transmission opportunity using the pseudo-random election algorithm. The node transmission intervals obtained from simulations are compared with the theoretical results.

## 4.2 Results

### 4.2.1 Transmission Interval

In the identical exponent case, all nodes have same transmission probability and expected holdoff time. However, the actual holdoff time depends on the channel contention situation. Fig.9 shows the expected node consecutive transmission intervals  $H + E[S]$  obtained from (18) and simulations under various node numbers and exponent values, where  $N$  is the total node number and  $x$  is the exponent value. We can see that the two sets of results match well. In the figure, the node transmission intervals increase with the total

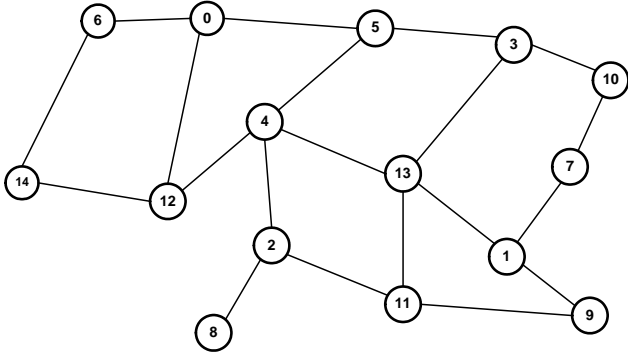


Figure 8: The node placement in general topology

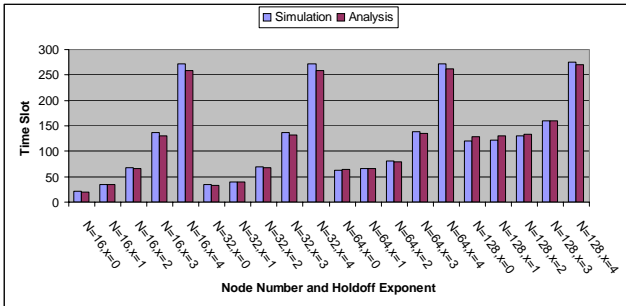


Figure 9: Simulation and analytical results on the expected transmission intervals for the identical exponent

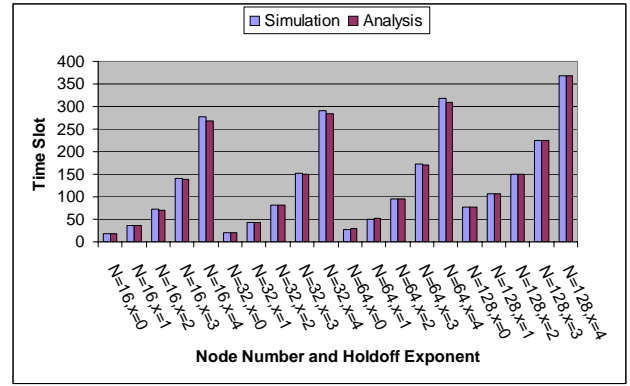


Figure 10: Simulation and analytical results on the expected transmission intervals for the nonidentical exponent

node number and exponent values. When  $N$  becomes larger, the contention becomes more intensive so that a node has to compete more times before it wins. When the exponent value increases, node holds off longer time before the next transmission, therefore the intervals increase with  $x$  too.

In the nonidentical exponent case, we divide the  $N$  nodes into five groups of equal size. The nodes in each group takes the same exponent value from the set  $\{0, 1, 2, 3, 4\}$ . The analytical transmission intervals obtained by (29) and the simulation results are shown and compared in Fig.10. Again the excellent match between the simulation and analysis demonstrates that our model is very accurate. It is seen that the system behaves similarly as in the identical exponent scenario, however the average of the intervals is longer.

In the 802.16 mesh mode, a node needs to compete for the next signaling channel access during the current one. Therefore, the interval between two consecutive transmissions is critical to the system performance. From the above results, we can conclude that the interval increases with the total neighbor number and exponent value. If there are more nodes in the neighborhood, the contention becomes intensive, so a node needs more time to get the access to channel. For different values of  $N$ , when  $x = 0$ , the competition is the most severe and a nodes fails many times before winning, especially when  $N$  is large. With the increase of the exponent value, the contention becomes less competitive because nodes have longer holdoff time; however, the transmission interval becomes longer too. We can also conclude that the exponent values have more significant impact on the system performance. Based on the results, a node with real-time traffic should have smaller exponent value so that it can have more chance to access the channel. On the other hand, too many nodes with small exponent values will generate serious contention. Hence a 802.16 system can be optimized by assigning appropriate exponent values to the nodes in the network.

#### 4.2.2 Three-way Handshaking Time

The IEEE 802.16 mesh mode employs a three-way handshaking procedure to set up connection. In this section, we compare the theoretical connection setup time obtained from (33) and (34) with that got by simulations. In our simulation, the pairs of requester and grantor are selected

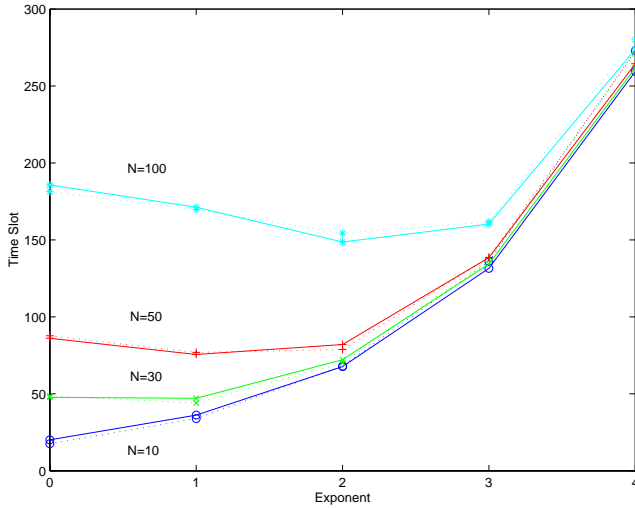


**Figure 11: Simulation and analytical results on the three-way handshaking time for the identical exponent case**

arbitrarily for the three-way handshaking and the results are the average of the data obtained from all pairs.

The three-way handshaking time for the identical exponent scenario is shown in Fig.11. In the simulation, the total node numbers are 10, 30, 50 and 100 respectively. The solid lines represent the theoretical results and the dotted lines are the data obtained by simulations. We can see that the two sets of results match very well. It is seen that the connection setup time increases with the total node number and exponent values. When  $N$  is large enough ( $N = 100$ ), the three-way handshaking time decreases first with the increase of exponent value and then goes up again. The reason is that the increase of  $x$  can reduce the channel competition to some extent when  $N$  is large. This phenomenon verifies our conclusion on the transmission interval. However, when the exponent  $x$  becomes large enough ( $x = 4$ ), the holdoff time dominates, hence, the connection setup time becomes similar under different number of nodes.

The three-way handshaking time for the nonidentical exponent scenario is also studied. Again we set the total node number to be 10, 30, 50 and 100. The total nodes are divided into five groups of equal size. The nodes in each group takes the same exponent value from the set  $\{0, 1, 2, 3, 4\}$ . Here, we present the cases for  $N = 10$  (Fig.12) and 100 (Fig.13) only. In these figures, the five pairs of curves are the connection setup time for requestors with exponent 0,1,2, 3, and 4 respectively. The abscissa represents the grantor exponent values. The solid lines are the analytical results and the dotted lines are the simulation results. Again it is seen that our model is very accurate for the nonidentical exponent scenario as well.

Different from the identical exponent case, the connection setup time for the nonidentical case is related with the requester and grantor order besides the exponent values. When two nodes with different exponent values want to set up a connection, according to the standard, if the node with smaller exponent value is the requester, the requester node has more chances to send confirmation message during the grantor's holdoff time after its reply. So the

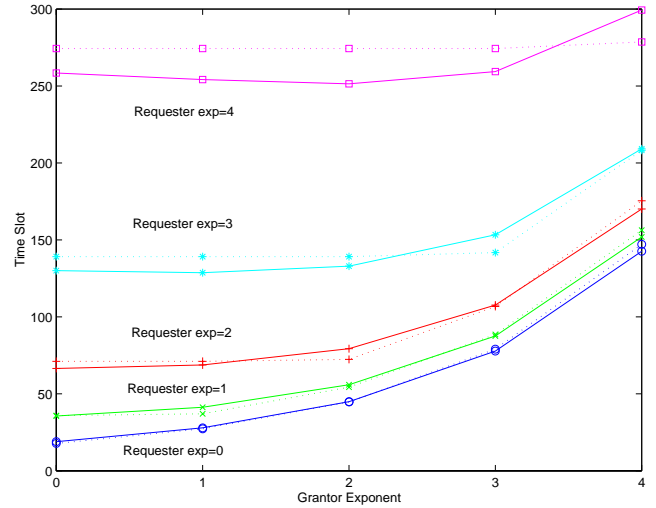


**Figure 12: Simulation and analytical results on the three-way handshaking time for the nonidentical exponent case with  $N = 10$**

connection setup time is shorter. On the other hand, the requester needs to hold off longer time before sending the confirmation message. In this case, the connection setup time is mainly decided by the requester's holdoff time. Because the requester's exponent value is large, the connection setup time becomes longer too. This point can be seen in the two figures. In the figures, we can also see that the connection setup time increases with the exponent values of the requester and grantor. The connection setup time also increases with the total node number. The curves for requestors with large exponent values are flatter, the reason is that the connection setup time is mainly determined by their eligible interval and holdoff time.

#### 4.2.3 General Topology Scenario

Table 1 shows the sequence numbers and the exponent values of each node in Fig.8. The node transmission intervals obtained by simulation and (32) are also included. The errors between simulation and theoretical results are less than 5%. This shows our model is accurate for general topology as well. Comparing with the collocated scenario, we can see that the node transmission intervals are similar. The reason is that although unknown nodes are always potential competitors in general topology, they can also be competing nodes in the collocated topology. The small variance of the total competing node number will not affect the system performance significantly.

## 5. CONCLUSIONS AND FUTURE WORK

In this paper, we have presented an analytical model for the distributed scheduling algorithm in the IEEE 802.16 mesh mode. In the mesh mode, every node competes for the channel access and tries to broadcast its scheduling information periodically. The channel contention result is correlated with the total node number, exponent value and network topology. Our model assumes that the transmit time sequences of all the nodes in the control subframe form statistically independent renewal processes. Based on this assumption, we have developed methods for estimating the

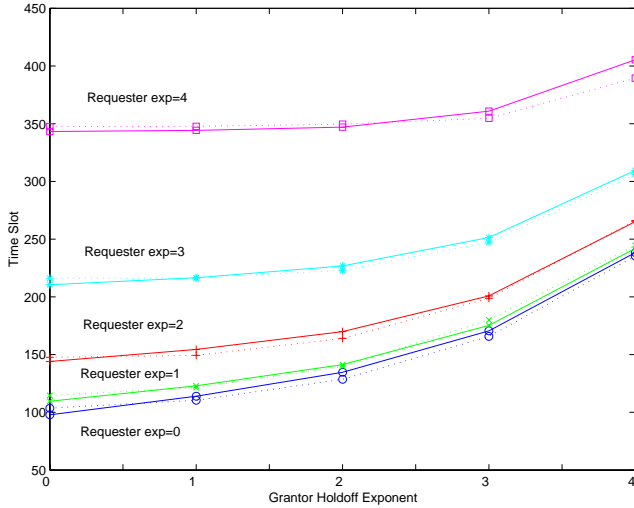


**Figure 13: Simulation and analytical results on the three-way handshaking time for the nonidentical exponent case with  $N = 100$**

Node	Exponent	Simulation	Analysis	Error
0	4	272.95	262.09	3.98%
1	0	18.52	18.65	0.66%
2	2	71.1	64.34	2.47%
3	3	138.78	134.48	3.12%
4	3	139.44	135.52	2.81%
5	1	38.23	37.91	0.85%
6	0	18.89	18.96	0.36%
7	2	70.76	69.14	2.28%
8	2	68.26	65.63	3.85%
9	1	36.36	36.05	0.86%
10	0	19.84	19.93	0.42%
11	3	138.86	134.29	3.29%
12	1	37.29	36.85	1.17%
13	0	21.12	21.53	1.96%
14	4	272.09	260.09	4.41%

**Table 1: Simulation and analytical results on the expected transmission intervals for the general topology**

distributions of the node transmission interval and connection setup delay, which are instrumental for evaluating performance like throughput and delay. Comparisons with ns-2 simulation results show that the model is quite accurate in typical scenarios.

Since the detail reservation scheme for the data subframe of the IEEE 802.16 mesh mode is left unstandardized, our model also sheds some light on the data subframe reservation scheme. For example, based on our analysis, the nodes with real time traffic shall have smaller holdoff exponents because they can have more chance to obtain data channel. However, too many nodes with small exponent value generate intensive competition that wastes system resource. Then the nodes can adjust their exponent values adaptively according to the competition node number variation to meet the connection QoS requirements. A good reservation scheme should guarantee the bandwidth allocation fairness and improve the channel utilization at the same time. Such a reservation scheme needs the information like the connection setup time and success probability provided by our model. Our future work is to propose such a reservation scheme taking into account the tradeoff between system resource utilization and the connection QoS requirements.

## 6. REFERENCES

- [1] IEEE P802.16-REVd/D5-2004. Part 16: air interface for fixed broadband wireless access systems. May 13, 2004.
- [2] Hikmet Sari. Trends and challenges in broadband wireless access. In *Communications and Vehicular Technology*, Oct, 2000.
- [3] Intel White Paper. IEEE 802.16 and WiMAX: broadband wireless access for everyone. July, 2003.
- [4] Nokia White Paper. Nokia rooftop wireless routing. June, 2003.
- [5] URL: [http://wirelessman.org/tga/contrib/C802.16a-02\\_30r1.pdf](http://wirelessman.org/tga/contrib/C802.16a-02_30r1.pdf)
- [6] Carl Eklund, Roger B. Marks, Kenneth L. Stanwood, and Stanley Wang. IEEE standard 802.16: a technical overview of the WirelessMAN™ air interface for broadband wireless access. In *IEEE Communication Magazine*, June, 2002.
- [7] Data-Over-Cable Service Interface Specifications, DOCSIS 2.0. Radio frequency interface specification. August, 2004.
- [8] Christian Hoymann, Markus Puttner, and Ingo Forkel. The HIPERMAN standard - a performance analysis. *IST SUMMIT 2003*.
- [9] Guosong Chu, Deng Wang, and Shunliang Mei. A QoS architecture for the MAC Protocol of IEEE 802.16 BWA System. *IEEE International Conference on Communications Circuits & System and West Sino Expositions*, vol.1, pp.435-439, China, 2002.
- [10] Kitti Wongthavarawat and Aura Ganz. IEEE 802.16 based last mile broadband wireless military networks with quality of service support. *IEEE Milcom 2003*, vol.2 pp.779-784.
- [11] J. Li, C. Blake, D. S. J. De Couto, H. I. Lee, and R. Morris. Capacity of ad hoc wireless networks. *ACM SIGMOBILE 2001*, Rome, Italy, pp.61-69.

- [12] P. Gupta and P. R. Kumar. The capacity of wireless networks. *IEEE Trans. on Information Theory*, vol. 46, no. 2, March 2003, pp. 388-404.
- [13] M. Gastpar and Martin Vetterli. On the capacity of wireless networks: the relay case. *IEEE Infocom 2002*, pp.1577-1586.
- [14] Y. C. Tay and K. C. Chua. A capacity analysis for the IEEE 802.11 MAC proposal. *Wireless Networks 7*, pp.159-171, 2001.
- [15] M. Grossglauser and D. N. C. Tse. Mobility increases the capacity of ad hoc wireless networks. *IEEE/ACM Trans. on Networksing*, vol. 10, no. 4, August 2002, pp. 477-486.
- [16] R. Negi and A. Rajeswaran. Capacity of power constrained ad-hoc networks. *IEEE Infocom 2004*.
- [17] Stavros Toumpis. Capacity bounds for three classes of wireless networks: asymmetric, cluster, and hybrid. *ACM MobiHoc 2004*, pp. 133-144.
- [18] G. Bianchi. Performance analysis of the IEEE 802.11 distributed coordination function. *IEEE J. Select. Areas Commun.*, vol. 18, no. 3, Mar. 2000.
- [19] F. Cali, M. Conti, and E. Gregori. Dynamic tuning of the IEEE 802.11 protocol to achieve a theoretical throughput limit. *IEEE/ACM Trans. on Networking*, vol. 8, no. 6, Dec. 2000.
- [20] F. Eshghi and A. K. Elhakeem. Performance analysis of ad hoc wireless LANs for real-time traffic. *IEEE/ACM Trans. on Networking*, vol. 21, no. 2, Feb. 2003.
- [21] H. Kim and J. C. Hou. Improving protocol capacity with model-based frame scheduling in IEEE 802.11-operated WLANs. *ACM MobiCom 2003*.
- [22] N. Gupta and P. R. Kumar. A performance analysis of the IEEE 802.11 wireless LAN medium access control. *Communications in Information and Systems*, vol. 3, no. 4, pp. 279-304, Sept. 2004.
- [23] T.-C. Houm L.-F. Tsao, and H.-C. Liu. Analyzing the throughput of IEEE 802.11 DCF scheme with hidden nodes. *IEEE VTC 2003*.
- [24] Samuel Karlin and Howard M. Taylor. A first course in stochastic processes. *Academic Press*, 1975.